2009 International Conference on Future Computer and Communication

A Comparison of UWB Communication Characteristics for Different Distribution of People and Various Materials of Walls

Min-Hui Ho
Department of Electrical Engineering
Tamkang University
Tamsui, Taipei, Taiwan, R.O.C.
nancy_2002_168@yahoo.com.tw

Shu-Han Liao
Department of Electrical Engineering
Tamkang University
Tamsui, Taipei, Taiwan, R.O.C.
shliao@ee.tku.edu.tw

Chien-Hung Chen
Department of Computer and Communication Engineering
Taipei College of Maritime Technology
Shilin, Taipei, Taiwan, R.O.C.
f1092@mail.tcmt.edu.tw

Chien-Ching Chiu
Department of Electrical Engineering
Tamkang University
Tamsui, Taipei, Taiwan, R.O.C.
chiu@ee.tuk.edu.tw

***Abstract*—A comparison of UWB communication characteristics for different distribution of people and various materials of walls in real environments are investigated. By using the impulse response of these multi-path channels, the mean excess delay, root mean square delay spread, and the number of multi-path arrivals within 10 dB of the peak multi-path arrival (NP10dB), and the number of paths required to meet the 85% energy capture threshold (NP(85%)) for these cases have been obtained. Numerical results have shown that the multi-path effect by people is an important factor for bit error rate (BER) and outage probability performance.**

Keywords-UWB, multi-path, bit error rate, outage probability

I. INTRODUCTION

UWB technology has received significant interests, particularly after the Federal Communications Commission (FCC)'s Report and Order in 2002 for unlicensed uses of UWB devices within the 3.1–10.6 GHz frequency band [1]. In this paper, a comparison of UWB communication characteristics for different distribution of people and various materials of walls in real environments are investigated. The effects of different materials of walls with wall board, concrete, limestone and iron on the UWB communication characteristics are presented. The different values of dielectric constant and conductivity of materials and people for different frequency are carefully considered in channel calculation. Results of this research provide valuable insights into the RMS delay spread and BER performance in the UWB communication system.

This paper aims at using SBR/Image method to simulate UWB communication system, and further compares their channel characteristics. In section II, a channel modeling and system description is presented. In section III, we show the numerical results. Finally, the conclusion is drawn in section Ⅳ.

II. CHANNEL MODELING AND SYSTEM DESCRIPTION

A. Calculation of the Channel Characteristics

The SBR/Image method can deal with high frequency radio wave propagation in the complex indoor environments [2], [3]. It conceptually assumes that many triangular ray tubes are shot from the transmitting antenna (TX), and each ray tube, bouncing and penetrating in the environments is traced in the indoor multi-path channel. If the receiving antenna (RX) is within a ray tube, the ray tube will have contributions to the received field at the RX, and the corresponding equivalent source (image) can be determined. By summing all contributions of these images, we can obtain the total received field at the RX. The depolarization yielded by multiple reflections, refraction and first order diffraction is also taken into account in our simulations.

The frequency responses are transformed to the time domain by using the inverse Fourier transform with the Hermitian signal processing [4]. By using the Hermitian processing, the pass-band signal is obtained with zero padding from the lowest frequency down to direct current (DC), taking the conjugate of the signal, and reflecting it to the negative frequencies. The result is then transformed to the time domain using IFFT [5]. Since the signal spectrum is symmetric around DC. The resulting doubled-side spectrum corresponds to a real signal in the time domain. The impulse response of the channel can be written as follows [6]:

$$h_{\mathrm{b}}(t) = \sum_{n=1}^{N} a_n \ \delta(t - \tau_n) \qquad (1)$$

where N is the number of paths observed at time. $\delta(.)$ is the Dirac delta function. a_n and τ_n are the channel gain and time delay for the n-th path respectively.

978-0-7695-3591-3/09 $25.00 © 2009 IEEE
DOI 10.1109/ICFCC.2009.129

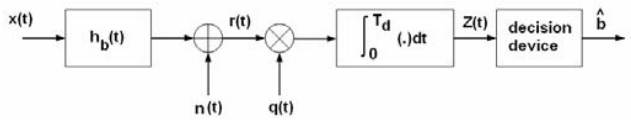

Figure 1. Block diagram of the simulated communication system.

B. System Block Diagram

The transmitted UWB pulse stream is [7]:

$$x(t) = \sqrt{E_{tx}} \sum_{n=0}^{\infty} p(t - nT_d)\, d_n \tag{2}$$

Where E_{tx} is the average transmitted energy and $p(t)$ is the transmitted waveform. T_d is the duration of the transmitting signal. $d_n \in \{\pm 1\}$ is a B-PAM symbol and is assumed to be independent identically distributed (i.i.d.). The transmitted waveform $p(t)$ is the second derivative Gaussian waveform with ultra-short duration T_p at the nanosecond scale. Note that T_p is the pulse duration and T_d is the duration of the transmitting signal. The value of T_d is usually much larger than that of T_p. The second derivative Gaussian waveform $p(t)$ can be described by the following expression:

$$p(t) = \frac{d^2}{dt^2}\left(\frac{1}{\sqrt{2\pi}\sigma} e^{\frac{-t^2}{2\sigma^2}}\right) \tag{3}$$

where t and σ are time and standard deviation of the Gaussian wave, respectively.

The average transmit energy symbol E_{tx} can be expressed as

$$E_{tx} = \int_0^{T_d} p^2(t)\,dt. \tag{4}$$

Block diagram of the simulated communication system is shown in Fig. 1. The received signal $r(t)$ can be expressed as follows:

$$r(t) = [x(t) \otimes h_b(t)] + n(t) \tag{5}$$

where $x(t)$ is the transmitted signal and $h_b(t)$ is the impulse response of the channel, $n(t)$ is the white Gaussian noise with zero mean and variance $N_0/2$. The correlation receiver samples the received signal at the symbol rate and correlates them with suitably delayed references given by

$$q(t) = p(t - \tau_1 - (n-1)T_d) \tag{6}$$

where τ_1 is the delay time of the first wave. The output of the correlator at $t = nT_d$ is [8], [9]:

$$\begin{aligned} Z(n) &= \int_{(n-1)T_d}^{nT_d} \left\{\left[\sqrt{E_{tx}} \sum_{n=0}^{\infty} p(t - nT_d) d_n\right] \otimes h_b(t)\right\} \cdot q(t)\,dt \\ &\quad + \int_{(n-1)T_d}^{nT_d} n(t) q(t)\,dt \\ &= V(t) + \eta(t) \end{aligned} \tag{7}$$

It can be shown that the noise components $\eta(t)$ of (7) are uncorrelated Gaussian random variable with zero mean. The variance of the output noise η is

$$\sigma^2 = \frac{N_0}{2} E_{tx}. \tag{8}$$

The conditional error probability of the Nth bit is thus expressed by:

$$P_e[Z(n)|\vec{d}] = \frac{1}{2} erfc\left[\frac{V(n)}{\sqrt{2}\sigma} \cdot (d_N)\right] \tag{9}$$

where $erfc(x) = \frac{2}{\sqrt{\pi}} \int_x^{\infty} e^{-y^2} dy$ is complementary error function and $\{\vec{d}\} = \{d_0, d_1, ..., d_N\}$ is the binary sequence.

Finally, the average BER for B-PAM IR UWB system can be expressed as

$$BER = \sum_{n=1}^{N} P(\vec{d}) \cdot \frac{1}{2} erfc\left[\frac{V(n)}{\sqrt{2}\sigma} \cdot (d_N)\right] \tag{10}$$

III. NUMERICAL RESULTS

The channel characteristics for different distribution of people and various materials of walls in the indoor environments are investigated. Fig. 2 is the top view of indoor environment with dimensions of 10m (Length) x 10m (Width) x 4.5m (Height).

These are four different distribution of people and four various materials of walls considered in the simulation. Four different numbers of people with 0, 4, 12 and 20 are simulated. Materials of walls with the wall board, concrete, limestone and iron are presented. 0.2m-thick floors and ceilings of the concrete are used for these cases. Note that the conductivity and dielectric constant of materials will change with the frequency in the UWB channel [10]-[12].

The transmitting antenna is located at Tx (5, 5, 3.5) m with the fixed height of 3.5m is located in the center of the indoor environment, as shown in Fig. 2. There are 361 receiving points for indoor environment. The locations of receiving antennas are distributed uniformly with a fixed height of 1m. The distance between two adjacent receiving points is 0.5m. Meanwhile, the receiver antenna located at Rx1 (1, 6, 1) m and Rx2 (5, 9, 1) m are also plotted in Fig. 2 for further discuss. The maximum number of bounces is set to be six and the first order diffraction is also considered in the simulation.

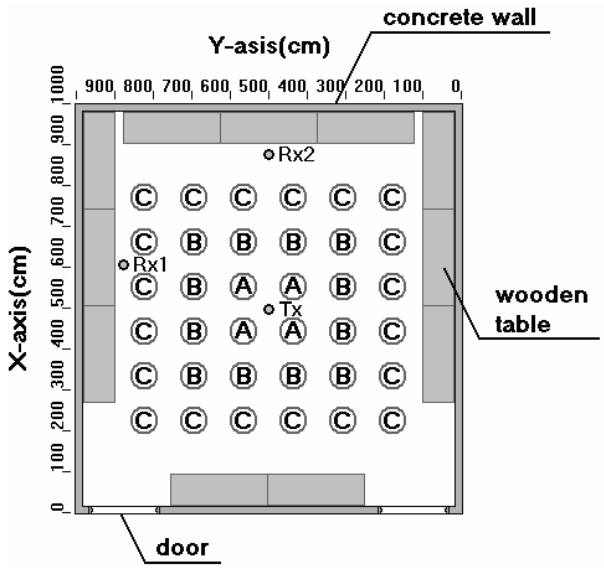

Figure 2. Top view of the indoor environment with dimensions of 10m (Length) x 10m (Width) x 4.5m (Height). Tx denotes the transmitter. Rx1, Rx2 are the receivers in three different locations. Marks "A", "B" and "C" are the positions of the people.

A. Different Distribution of People

In the Fig. 2, there are four people in the position marked "A" where each "A" represents one person. Similarly, there are twelve people on the position marked "B". Finally, there are twenty people on the position "C".

Fig. 3 shows the cumulative distribution function of RMS delay spreads for different distribution of people. It is seen that the RMS delay spread value for 20 people is most serious due to the multi-path effect caused by people.

The BER versus signal-to-noise rate (SNR) for receivers at Rx1 is plotted in Fig. 4. Here SNR is defined as the ratio of the average power to the noise power at the front end of the receiver. For a BER requirement of 10^{-6}, the SNR value for 20 people is larger about 4dB than that without people.

At 100M bps transmission rate and for a BER $<10^{-6}$, the outage probability versus SNR are calculated, as shown in Fig. 5. It is seen that the outage probabilities at SNR=16dB are about 16% and 1% for the 20 people and without people respectively. It is clear that the BER performance without people is better due to the less severe multi-path effect.

Table I shows channel characteristics for different distribution of people. The number of people with 0, 4, 12 and 20 are considered. It is found that the values of RMS delay spread, Mean excess delay, NP(85%) and NP10dB increase as the number of people increase. The mean RMS delay spread without people is 17.50ns and increases about 32% to 23.15ns for the 20 people. It is clear that the multi-path effect is severe when the number of people increases. It is also seen that the mean excess delay without people is 11.43ns and increases about 69% to 19.34ns for the 20 people. Similarly, NP10dB and NP(85%) also increase a lot for 36 people.

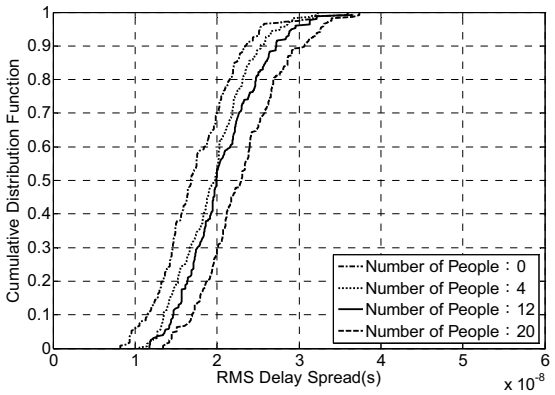

Figure 3. Cumulative distribution of RMS delay spreads for the different distribution of people

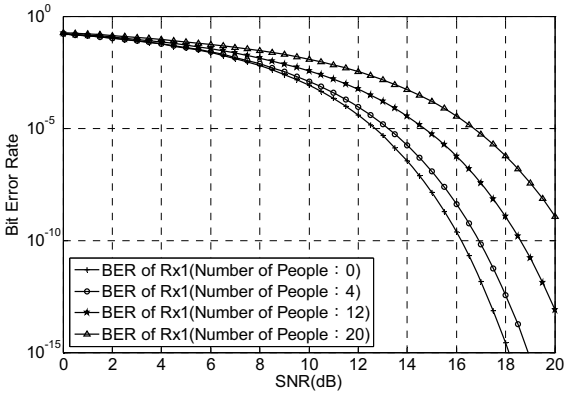

Figure 4. BER versus SNR for the different distribution of people

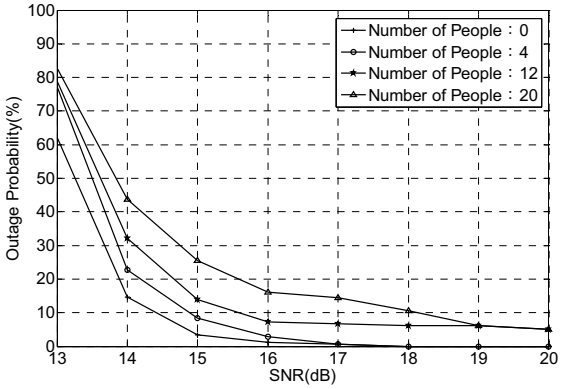

Figure 5. Outage probability versus SNR for different distribution of people

TABLE I. PARAMETERS OF MULTI-PATH CHANNELS FOR DIFFERENT DISTRIBUTION OF PEOPLE

	RMS Delay Spread (ns)		Mean Excess Delay (ns)		NP10dB	NP(85%)
Number of People	***Mean***	***Standard deviation***	***Mean***	***Standard deviation***	***Mean***	***Mean***
0	17.50	5.06	11.43	4.05	5.56	33.82
4	19.51	4.50	12.83	5.65	5.78	37.94
12	20.65	4.90	16.60	9.70	6.96	50.27
20	23.15	5.13	19.34	10.36	7.70	63.08

B. Various Materials of Walls

Four materials of walls with wall board, concrete, limestone and iron are considered. The position of transmitting and receiving antennas are the same as the previous one except that the room is empty now. In other word, there is no people and furniture. 0.2m-thick floors and ceilings of the concrete are used for these cases. UWB channel characteristics in the indoor environment with different materials of walls are investigated.

Fig. 6 shows the cumulative distribution function of RMS delay spreads for various materials of walls. It is seen that the RMS delay spread value for wall with iron materials is more serious than the other materials of walls. The BER versus signal-to-noise rate (SNR) for receivers at Rx2 is plotted in Fig. 7. For a BER requirement of 10^{-6}, the SNR value for iron wall is larger about 4 dB than that for wall board. At 100M bps transmission rate and for a BER $<10^{-6}$, the outage probability versus SNR are calculated, as shown in Fig. 8. It is seen that the outage probabilities at SNR=16dB are about 79% and 1% for the iron wall and wall board respectively. It is clear that the BER performance for wall board is better due to the less severe multi-path effect.

Table II shows channel characteristics for these four various materials of walls. There are four parameters, including RMS delay spread, Mean excess delay, NP10dB and NP(85%). It is clear that the values of RMS delay spread, Mean excess delay, NP(85%) and NP10dB for iron walls are the largest due to the strong reflection. Note that the value of RMS delay spread for iron walls is more than twice as that for wall of the other materials. It is also found that the mean excess delay increases from about 11.95ns for the concrete walls to about 51.18ns for the iron walls. Similarly, NP(85%) and NP10dB increase a lot for the iron walls. This situation can be explained by the fact that the multi-path effect for the iron walls is very severe due to the total reflection. Besides, it is seen that the values of RMS delay spread, Mean excess delay, NP(85%) and NP10dB for the wall board, concrete and limestone are almost the same.

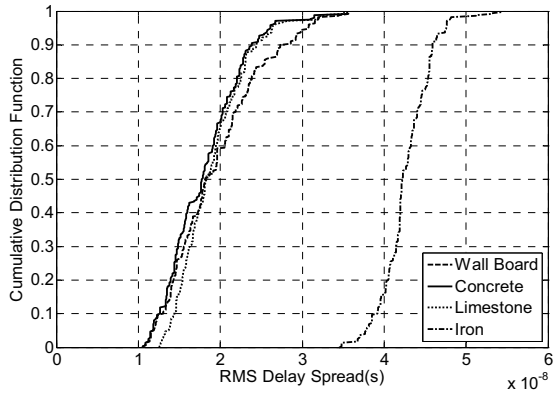

Figure 6. Cumulative distribution of RMS delay spreads for the various materials of walls

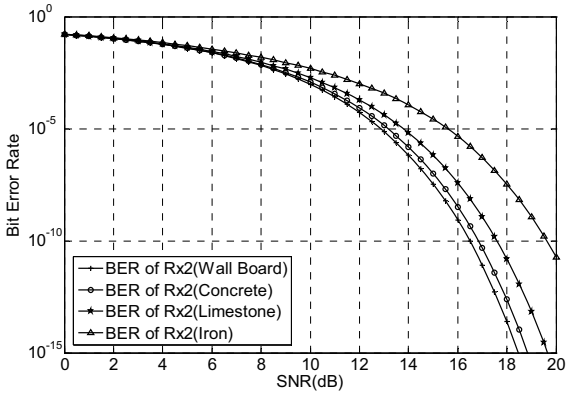

Figure 7. BER versus SNR for the various materials of walls

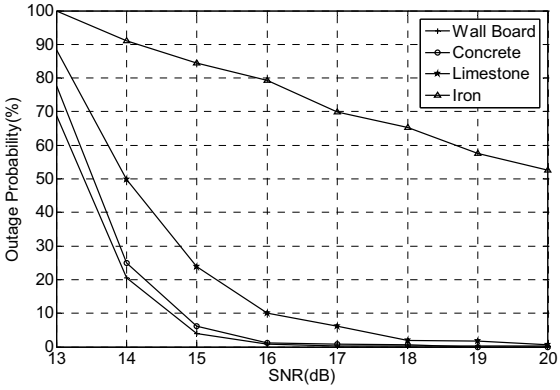

Figure 8. Outage probability versus SNR for various materials of walls

TABLE II. PARAMETERS OF MULTI-PATH CHANNELS FOR VARIOUS MATERIALS OF WALLS

	RMS Delay Spread (ns)		Mean Excess Delay (ns)		NP10dB	NP(85%)
Materials of Wall	***Mean***	***Standard deviation***	***Mean***	***Standard deviation***	***Mean***	***Mean***
Wall Board	19.45	5.67	12.50	5.81	5.62	40.09
Concrete	18.14	4.75	11.95	4.33	5.69	37.37
Limestone	19.08	4.29	15.13	5.48	7.29	61.22
Iron	42.65	3.03	51.18	9.52	27.12	364.19

IV. CONCLUSIONS

A comparison of UWB communication characteristics for different distribution of people and various materials of walls are presented. The values of the RMS delay spread vary with different distribution of people. Numerical results show that the values of RMS delay spread, Mean excess delay, NP(85%) and NP10dB increase as the number of people increase. Moreover, the outage probabilities for 100 Mbps B-PAM and for a BER $<10^{-6}$ versus SNR are calculated. It is found that the outage probability for the 20 people is the largest. The performance of outage probability with people is worse than that without people in UWB environment. This is due to the multi-path effect is severe when people exist in the room.

Four materials of walls with wall board, concrete, limestone and iron wall are considered. The RMS delay spreads for iron wall are largest due to the strong multi-path effect. The BER performance for B-PAM UWB indoor communication with various materials of walls has been investigated. Numerical results show that outage probabilities for the UWB multi-path environment with iron wall are larger than those for the other wall. The multi-path effect is severe for the iron wall due to the total reflection.

ACKNOWLEDGMENT

The authors would like to acknowledge the many helpful suggestions of anonymous reviewers.

REFERENCES

[1] Rui Xu, Yalin Jin, and Cam Nguyen, "Power-Efficient Switching-Based MOS UWB Transmitters for UWB Communications and Radar Systems," *IEEE Transactions on Microwave Theory and Techniques,* Vol. 54, pp. 3271-3277, Aug. 2006.

[2] S. H. Chen and S. K. Jeng, "An SBR/Image Approach for Indoor Radio Propagation in a Corridor," *IEICE Trans. Electron*., Vol. E78-C, pp. 1058-1062, 1995.

[3] S. H. Chen and S. K. Jeng, "SBR/Image Approach for Indoor Radio Propagation in Tunnels With and Without Traffic," *IEEE Trans. Veh. Technol*., Vol. 45, pp. 570-578, 1996.

[4] I. Oppermann, M. Hamalainen, and J. Iinatti, *UWB Theory and Applications*, John Wiley & Sons, 2004

[5] E. W. Kamen and B. S. Heck, *Fundamentals of Signals and Systems Using the Web and Matlab*, Prentice-Hall, 2000.

[6] M. Gabriella, D. Benedetto, and G. Giancola, *Understanding Ultra Wide Band Radio Fundamentals*, Prentice Hall, 2004.

[7] Zhi Tian and G. B. Giannakis, "BER sensitivity to mistiming in ultra-wideband impulse Radios-part I: nonrandom channels," *IEEE Transactions on Signal Processing,* pp. 1550 - 1560, Apr 2005.

[8] E. A. Homier and R. A. Scholtz, "Rapid acquisition of ultra-wideband signals in the dense multi-path channel," *IEEE Conference on Ultra Wideband Systems and Technologies,* pp. 105 – 109, 2002.

[9] D. J. Gargin, "A fast and reliable acquisition scheme for detecting ultra wide-band impulse radio signals in the presence of multi-path and multiple access interference" *2004 International Workshop on Ultra Wideband Systems,* pp. 106 - 110, May 2004.

[10] Yan Zhao, Yang Hao, Akram Alomainy, and Clive Parini, **"**UWB on-body radio channel modeling using ray theory and subband FDTD method**,"** *IEEE Transactions on Microwave Theory and Techniques*, Vol. 54, pp. 1827-1835, June 2006

[11] R. Michael Buehrer, Ahmad Safaai-Jazi, William Davis, and Dennis Sweeney, "Ultra-wideband Propagation Measurements and Modeling Final Report," *DARPA NETEX Program Virginia Tech*, Chapter 3, pp. 38-216, Jan 2004

[12] A. Muqaibel, A. Safaai-Jazi, A. Bayram, A.M. Attiya and S.M. Riad, "Ultrawideband through-the-wall propagation," *IEE Proceedings Microwaves, Antennas and Propagation*, pp. 581-588, Dec. 2005.